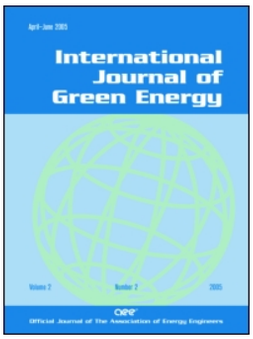

International Journal of Green Energy

ISSN: 1543-5075 (Print) 1543-5083 (Online) Journal homepage: www.tandfonline.com/journals/ljge20

The effect of pyrolysis atmosphere on bio-oil yields and structure

Eylem Önal, Başak Burcu Uzun & Ayşe Eren Pütün

To cite this article: Eylem Önal, Başak Burcu Uzun & Ayşe Eren Pütün (2017) The effect of pyrolysis atmosphere on bio-oil yields and structure, International Journal of Green Energy, 14:1, 1-8, DOI: 10.1080/15435075.2014.952421

To link to this article: https://doi.org/10.1080/15435075.2014.952421

INTERNATIONAL JOURNAL OF GREEN ENERGY
2017, VOL. 14, NO. 1, 1–8
http://dx.doi.org/10.1080/15435075.2014.952421

Taylor & Francis
Taylor & Francis Group

The effect of pyrolysis atmosphere on bio-oil yields and structure

Eylem Önal[a], Başak Burcu Uzun[b], and Ayşe Eren Pütün[b]

[a]Faculty of Engineering, Chemical and Process Engineering, Bilecik Seyh Edebali University, Bilecik, Turkey; [b]Department of Chemical Engineering, Anadolu University, Iki Eylul Campus, Eskisehir, Turkey

ABSTRACT

A food industry waste, almond shell, was pyrolyzed under three different environment static, nitrogen, and steam to produce bio-oil and its derivatives. The oil yield obtained at pyrolysis temperature of 600°C was 24.23% in a static atmosphere, whereas it increased to 27.25% and 33.05% in nitrogen and steam atmospheres, respectively. The bio-oil obtained under steam atmosphere is very efficient due to the production of high liquid and gas yields. Moreover, co-feeding steam during the pyrolysis altered the bio-oil structure by increasing the aliphatics and reducing the asphaltenes. Moreover, steam treatment also increases H/C and heating value of bio-oils. According to the obtained results, steam pyrolysis is an alternative option for future applications in refineries.

ARTICLE HISTORY
Received 11 May 2013
Accepted 4 August 2014

KEYWORDS
Almond shell pyrolysis; bio-oil production; steam pyrolysis

Introduction

The pyrolysis of organic waste streams is a promising method to obtain both energy and chemicals. It is an anaerobic thermal degradation process in which biomass is converted to renewable energy feed stocks either gas, liquid, or solid. Being an alternative for fuel oil or diesel in many static applications for heat or electricity generation (boilers, furnaces, engines, and turbines), development of an economic process for bio-oil production is very important. Moreover, its energy density is four to five times higher than the original solid material by offering important logistic advantages. By deriving more energy from biomass feedstock, many countries might be able to decrease their reliance on imported petroleum (Bridgewater, Meier, and Radlein 1999; Uzun, Pütün, and Pütün 2007; Cornelissen et al. 2009). Pyrolysis is considered as one way for the high oxygen content biomass assessment because high value gas, liquid products like fuel or chemical materials and good quality chars are obtained (Wang et al. 2010; Zhang et al. 2010; Jin et al. 2012; Fukuda 2015).

There are many studies about pyrolysis (activated carbon production), gasification, and combustion of almond shells but there are a few about steam pyrolysis of almond shells, which are focused on liquid production (Font et al. 1986; Font et al. 1995; Caballero, Font, and Marcilla 1996; Jenkins et al. 1996; Gonzalez et al. 2005; Demirbaş 2006; Mohan et al. 2011; Nabais et al. 2011). Presence of steam in the pyrolysis favors the formation of high yield of liquid products, while the almost simultaneous pyrolysis and gasification of the fuel results in formation of solid product with high surface area and well-developed porous structure. In addition, steam pyrolysis is beneficial not only for the development of pore structure of activated carbon, but also for the improvement of low molecular weight compounds, namely, liquid yields. It can be beneficial for upgrading units in refineries (Minkova et al. 1991, 2001; Ekinci and Yurum 1995; Savova et al. 2001).

In this study, almond shells are selected as feedstock for bio-fuel and value-added chemicals production and the aims of the study are determination of the effect of pyrolysis atmosphere either static, nitrogen, or steam, on product yields, and evaluation of the liquid product as conventional fossil fuels or chemical feed stocks.

Experimental study

Raw material

Turkey has a share of 3.5% in the world shelled almond production and 44,366 tons of almonds and 23,205 tons of almond shells are produced annually (Gokcol et al. 2009). Therefore, almond shell generated by the product of almond production is chosen as the biomass sample. The sample was taken from the city Mugla-Datca located in Aegean region, western part of Turkey. The results of proximate and ultimate analyses are given in Table 1. Air-dried samples were grounded in a high-speed rotary cutting mill and screened to give fractions of Dp > 1.8 mm; 1.8 > Dp > 0.85 mm; 0.85 > Dp > 0.425 mm; Dp < 0.425 mm, 0.425 < Dp < 0.224, 0.224 < Dp. Average particle size was found to be as 1.67 mm. Proximate analysis was performed on the sample to determine the weight fractions of moisture, volatile, ash, and fixed carbon contents. The ASTM Standard E 870-82 was used. The average bulk density of the almond shell sample was found to be as 730 kg m^{-3} according to ASTM 321-D. The ultimate analysis was performed in an elemental analyser (Carlo Erba, EA 1108). The other properties of almond shell are also given in Table 1. The protein content of the

CONTACT Başak Burcu Uzun and Ayşe Eren Pütün aeputun@anadolu.edu.tr Department of Chemical Engineering, Anadolu University, Iki Eylul Campus, 26555 Eskisehir, Turkey.

Table 1. Main characteristics of almond shell.

Proximate analysis (wt.%, as received)	
Moisture	8.80
Volatiles	72.00
Fixed C	17.63
Ash	1.34
Elemental analysis (wt.%. daf basis[a])	
Carbon	50.2
Hydrogen	5.76
Nitrogen	0.18
Oxygen (by difference)	43.90
Empirical formula	$CH_{0.73}N_{0.003}O_{0.66}$
H/C molar ratio	0.73
O/C molar ratio	0.66
Calorific value (MJ kg^{-1})	17.29
Component analysis (wt.%, as received)	
Extractives	12.92
Hemicellulose	24.37
Lignin	28.50
Cellulose	31.88
Oil	8.50
Protein	1.51
Holocellulose	56.25

[a]Dry and ash free.

sample was determined by the Kjeldahl method (ASTM E-258-67) using Labconco Rapid still-2. Thermogravimetric analysis (TGA) was applied using LINSEIS Thermowaage L 81 coupled with differential thermal analyzer (DTA). The sample, weighing approximately 20 mg, was heated to 1200°C with a heating rate of 10°C min^{-1} under nitrogen atmosphere (100 cm^3 min^{-1}).

Pyrolysis experiments

The pyrolysis of the air-dried almond shell samples was carried out in a fixed-bed reactor in three different atmospheres, namely, static, nitrogen, and steam as the carrier gas. The 316 stainless steel retort has a volume of 400 cm^3 (70 mm i.d.) and is externally heated by an electric furnace in which the temperature is measured by a thermocouple inside the bed. The connecting pipe between the reactor and the trapping system was heated to 400°C to avoid condensation of the pyrolysis vapor.

For the first part of the pyrolysis experiments, 10 g sample of almond shell was placed into the reactor and pyrolyzed at 400°C, 450°C, 500°C, 550°C, 600°C, 700°C with a heating rate of 5°C min^{-1}. In the second part of the experiments, the sample was pyrolyzed at 600°C under nitrogen atmosphere with a flow rate of 50, 100, 200, 400 cm^3 min^{-1} and with a heating rate of 5°C min^{-1}. The flow of gas released was measured using a soap film for the duration of experiments. The liquid phase was collected in cold traps maintained at about 0°C using salty ice. The liquid phase was consisted of aqueous and oil phases that were separated by decanting at room conditions and then weighed. After pyrolysis, the solid char was removed and weighed, and then gas yield was calculated by the difference.

The last group of experiments was established to investigate the effect of steam. Pure steam at 10 psig was sent to reactor from a generator and the linear velocity of the steam is calculated according to the inlet diameter of reactor (0.63 cm). Keeping all the parameters constant as previous parts, only steam velocity was changed as 0.6, 1.3, and 2.7 cm s^{-1}.

Structural analyses

Elemental analyses were applied on bio-oil samples for elemental composition and calorific value. The chemical class compositions of the oils were determined by liquid column chromatography technique. The oils were first separated into n-pentane soluble and insoluble compounds (asphaltenes), of which the n-pentane soluble compounds were further separated by adsorption chromatography. Glass column used was packed with silica gel 70–230 mesh, pre-treated at 105°C for 2 h prior to use. The column was eluated successively with 150 mL n-pentane, 200 mL toluene, and 200 mL methanol to produce aliphatic, aromatic, and polar subfractions, respectively. Each fraction was dried and weighed. The Fourier transform infrared (FTIR) spectroscopy of the bio-oils and subfractions was achieved on thin films between KBr plates by using Bruker Tensor 27 Fourier Transform Infrared Spectrophotometer. Gas chromatography–mass spectrometry (GC–MS) analysis of the aliphatic subfraction was analyzed with an HP 6890 gas chromatograph equipped with 5793 mass selective detector using an HP-5 capillary column supplied from Hewlett-Packard, USA. The following temperature program was used: initial and final temperatures were 40°C and 280°C, respectively, retention times at initial and final temperatures were both 10 min and the heating rate was 8°C min^{-1}. The ^1H nuclear magnetic resonance (NMR) of oils was obtained at an H frequency of 500 MHz using a Bruker BioSpin GmbH instrument. The sample was dissolved in chloroform-*d*.

Result and discussion

The results for the proximate analysis of almond shell are shown in Table 1. Due to having less ash content and higher fixed carbon, almond shell seems to be a promising raw material for thermo-chemical conversions. Calorific value of almond shell was calculated as about 17.29 MJ kg^{-1} with Du-Long's formula according to elemental analysis results (Harker and Backhurst 1981).

TGA is one of the major thermal analysis techniques used to study the thermal behavior of carbonaceous materials. It is important to determine the thermal degradation stages during the devolatilization (Williams and Besler 1992; Uzun, Pütün, and Pütün 2007). The thermal degradation characteristics, TG, and DTG curves of the almond shell are shown in Figure 1. The mass loss (7.46 wt.%) till 200°C is associated with evaporation of moisture adsorbed on samples. Devolatilization began at about 220°C and the removal of volatiles was completed at about 1100°C. After that, there is no further loss of weight essentially. The main decomposition of the biomass (~60.48%) occurred at the temperature range between 200°C and 400°C. After this temperature, devolatilization rate was decreased. The decomposition of biomass was 21.23% (400°C–650°C) and 13.02% (650°C–1100°C). After this temperature range, there was no mass change. The sharp peak at 288.9°C represents hemicellulose decomposition and the other sharp peak at 345.4°C belongs to the cellulose decomposition. This implies that the main pyrolysis reactions including depolymerization, decarboxylation, and cracking

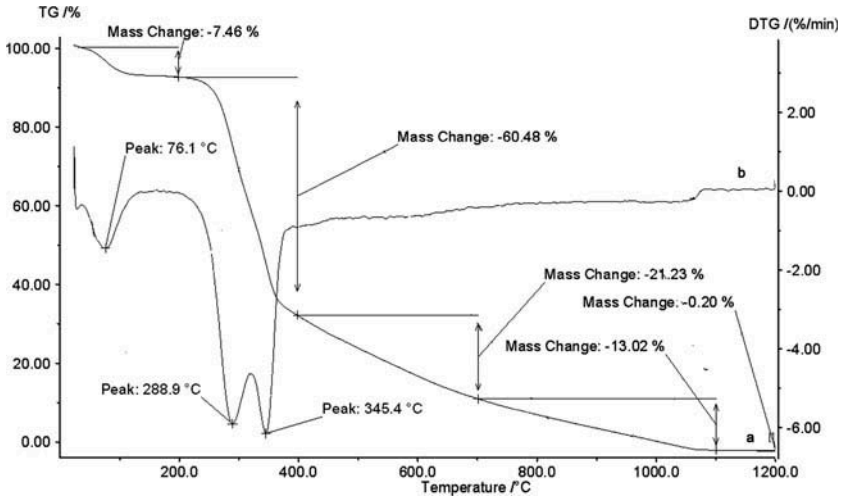

Figure 1. TG (a) and DTG (b) of almond shell sample.

take place over the given temperature range. The lower temperature of DTG peak of almond shell mainly represents the moisture, while the higher temperature of DTG peak represents degradation of hemicellulose and cellulose, which cause the formation of organic volatiles, whereas devolatilization of lignin enhances the formation of char. Lignin decomposition occurred throughout the temperature in the range of 200°C–1100°C, but the main area of weight loss occurs at higher temperatures.

To have information about the chemical structure of almond shell, FTIR spectrum is taken and given in Figure 2. It shows that chemical structure of the sample, being a lignocellulosic material, is made up of different atomic groupings and a large number of functional groups. The broad and flat band at about 3350 cm^{-1} is ascribed to OH stretching vibrations in hydroxyl groups, which is attributed to lignin structure and moisture content of the sample. Two very strong bands at 2925 and 2855 cm^{-1} are assigned to C–H stretching vibrations in CH_2 groups and a weak band at 1453 cm^{-1} due to C–H deformation frequencies confirms the presence of these functional groups. The next strong band (1742 cm^{-1}) is ascribed to C=O vibrations probably from esters, ketones, or aliphatic acids. At 1615 cm^{-1}, the very strong band is assigned to either C=C conjugated, aromatic conjugated, or C=N conjugated or cyclic double bond vibrations. Skeletal vibrations from $(CH_3)_3$–C–R give a strong band at 1246 cm. The weaker bands between 880 and 600 cm^{-1} are ascribed to aromatic structures (Bellamy 1975; Duran-Valle et al. 2005; El-Hendawy 2006).

Figure 3 shows the product yields of almond shell at a constant heating rate of 5°C min^{-1}, with respect to final temperatures of 400°C, 450°C, 500°C, 550°C, 600°C, and 700°C. As seen from Figure 3, increasing temperature increased the gas yield while decreasing the char yield. For instance, the gas yield increased from 44.99% to 48.37%, and the char yield decreased from 31.41% to 28.12%, when the final pyrolysis temperature was raised from 400°C to 700°C. The oil yield was 18.93% at a pyrolysis temperature of 400°C, it appeared to go through a maximum of 24.23% at the temperature of 600°C. Then, at the final temperature of 700°C, the oil yield decreased to 19.96%. As seen, an increase of temperature after 600°C favors the gasification reactions, hence lower quantity of oil is obtained at high temperatures. Previous workers reported that the optimum pyrolysis temperature for maximizing the oil yield lay in the temperature

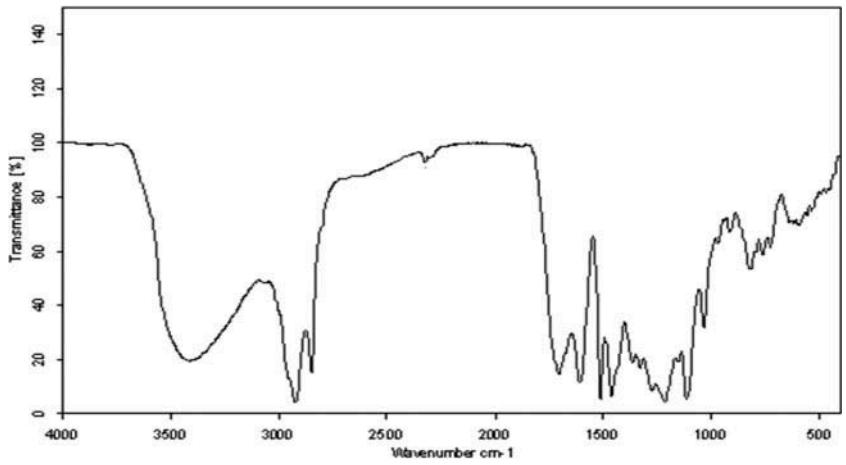

Figure 2. FTIR spectra of almond shell.

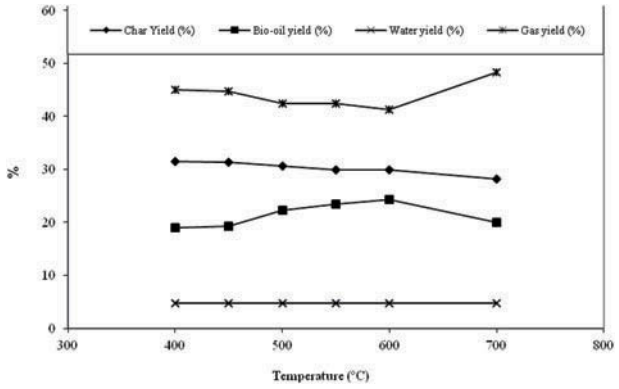

Figure 3. Pyrolysis of almond shell at different temperatures, product yields.

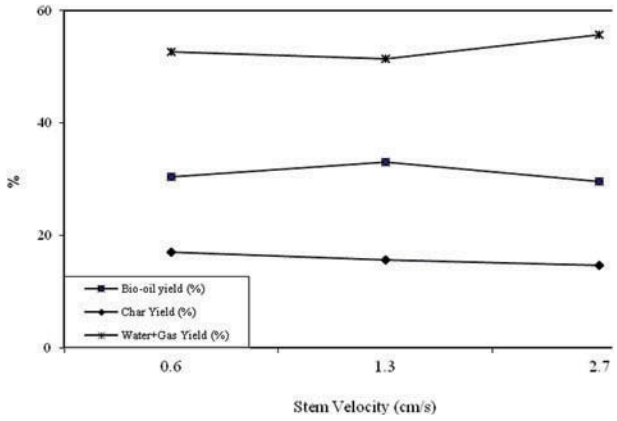

Figure 5. Pyrolysis of almond shell at different steam velocities, product yields.

range between 500°C and 600°C (Vitolo et al. 1999; Pütün, Özcan, and Pütün 1999; Encinar, Gonzales, and Gonzales 2000; Pütün, Uzun, and Pütün 2006). Our results are consistent with the previous workers. It can be concluded that at higher temperatures above the optimum, the amount of bio-oil decreases due to gasification reactions, so higher temperatures are favored for obtaining gaseous products.

At the optimum pyrolysis temperature (600°C), the second set of pyrolysis experiments was conducted to determine the effect of sweeping gas (N_2) at different flow rates (50, 100, 200, and 400 cm^3 min^{-1}) with a heating rate of 5°C min^{-1}. The results of the experiments are given in Figure 4. The oil yield reached its maximum of 27.25% with a sweeping gas flow of 200 cm^3 min^{-1}. Use of sweeping gas caused a 12.50% increase in oil yield in comparison with the maximum yield found in the first set. The nitrogen flow affects the residence time of the vapor phase produced by pyrolysis so that higher flow rates cause rapid removal of products from the reaction medium and minimize secondary reactions such as char formation (Pütün, Uzun, and Pütün 2006). However, increasing the nitrogen flow rate more than 200 cm^3 min^{-1} caused a reduction in liquid yields in the present reaction conditions. As seen from Figure 4, the gas yield rises with increasing nitrogen flow rate whereas the char yield decreases; because uncondensed volatiles are removed from the reaction zone by the nitrogen stream.

Experimental results are given in Figure 5. The bio-oil yield obtained in static atmosphere increased from 24.23% to 33.05% under steam atmosphere. As seen, both bio-oil and gas yields increase under steam atmosphere with comparison to both nitrogen and static atmospheres. Savavo et al. reported that the presence of water vapor during pyrolysis leads to a considerable increase in the liquid and gas product yields in addition to reducing the sulfur content in liquid and solid products (Savova et al. 2001). These results are explained by Minkova et al., who reported that the water vapor is not only an implement for volatiles but also a reactive agent, which reacts with the pyrolysis product and may stabilize the radicals obtained in the thermal decomposition of the fuel increasing the yield of volatiles (Minkova et al. 1991, 2001).

Use of steam caused reduction of solid yields. The lowest yield of solid residue was obtained as 14% under steam atmosphere in comparison with static and nitrogen atmospheres. This can be explained by the ability of the water vapor to penetrate the solid material and to help in desorption, distillation, and efficient removal of the volatile products from it. During pyrolysis in the static and nitrogen atmospheres, some of the pores in the solid material may be blocked by deposition of carbonaceous material and this contributes also to higher yield of the solid residue (Minkova et al. 1991, 2001).

The elemental compositions of oils derived from pyrolysis of almond shell under various atmospheres are compared with diesel and heavy fuel oil and results are given in Table 2. As seen from the table, the significant decrease in oxygen content of the oil (24.46%) compared to the original feedstock (43.90%) was found. This is significant, because the high oxygen content is not attractive for the production of transport fuels. The bio-oils from biomass usually contain higher proportion of oxygen than fossil oil, and thus they

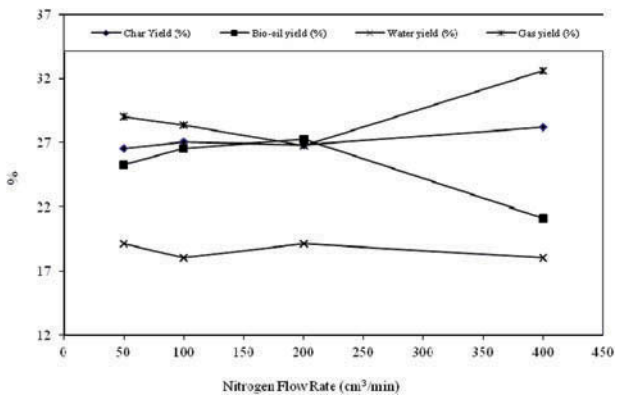

Figure 4. Pyrolysis of almond shell at different nitrogen flow rates, product yields.

Table 2. The comparison of almond shell bio-oil, diesel, and heavy fuel oil.

Component	AS[1]	AS[2]	AS[3]	Diesel[27]	Heavy fuel oil[27]
C	66.79	63.85	67.48	86.58	85–86
H	8.75	8.60	9.96	13.29	11–11.5
N	–	0.17	0.18	65 ppm	0.3–0.5
S	–	–	–	0.11	1.0–2.6
O[a]	24.46	27.75	22.38	0.01	–
H/C	1.57	1.62	1.76	1.84	1.55–1.62
HHV (MJ kg^{-1})	34.87	35.42	33.16	45.50	42–43

[a]By difference. [b]Mohan et al., 2006.
AS: pyrolysis oil from almond shell from [1]static, [2]nitrogen, and [3]steam atmosphere.

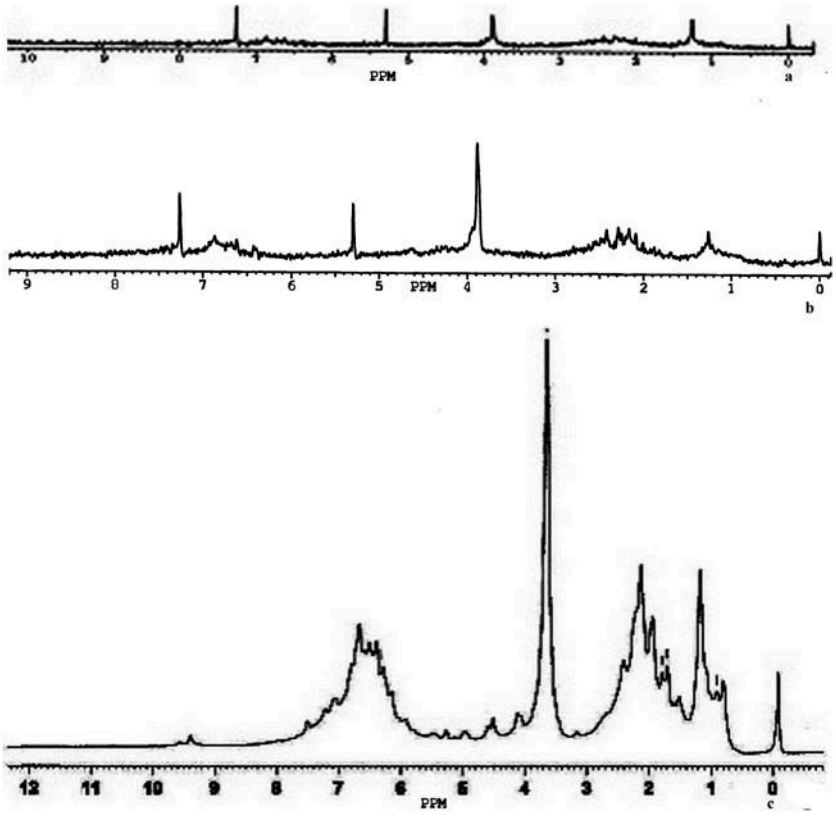

Figure 6. Proton NMR spectra for bio-oils under (a) static, (b) nitrogen atmosphere, and (c) steam atmosphere.

are quite reactive and not as stable as fossil fuels. Therefore, characteristics of bio-oils change rapidly during condensation and under storage conditions. Their utilization as fuels or sources of chemical feedstock requires some form of upgrading to improve storage stability and heating value (Önal, Uzun, and Pütün 2011). Further comparison of H/C ratios with conventional fuels indicates that H/C ratios of the oils obtained in this study is similar to light and heavy petroleum products. Moreover, steam treatment during the pyrolysis increases both H/C ratio and higher heating value (HHV) of oils.

The ^{1}H NMR spectra of the static, nitrogen, steam bio-oils, and hydrogen distributions are given in Figure 6 and Table 3, respectively. According to Table 3, bands between 0.5 and 3.0 ppm were identified as aliphatics. The signal due to the oxygenated phenols, the 4–6 ppm range, was broadened. Resonances between 6 and 9 ppm were assigned to aromatic structures. The aromatic content of static pyrolysis oil (13%) was increased to 15.58% with nitrogen atmosphere pyrolysis. The maximum aromatic content was obtained with steam pyrolysis. These findings were consistent with the results of column chromatography.

Table 3. Results of ^{1}H NMR for the bio-ils from the pyrolysis of almond shell obtained under three atmospheres at 600°C.

Hydrogen type	Chemical shift (ppm)	Static (%)	Nitrogen (%)	Steam (%)
CH_3 γor further from aromatic ring and paraffinic CH_3	1.0–0.5	_	_	6.10
CH_3; CH_2 and CH β to aromatic ring	1.5–1.0	22.03	4.28	9.13
CH_2 and CH attached to naphthenes	2.0–1.5	_	_	17.06
CH_3; CH_2 and CH α to aromatic or acetylenic	3.0–2.0	45.00	44.44	13.79
Total aliphatics	3.0–0.5	67.03	48.72	46.08
Hydroxyl, ring-joining methylene, methane, or methoxy	4.0–3.0	12.19	27.18	21.93
Phenols, non-conjugated olefins	6.0–4.0	7.81	8.51	4.50
Aromatics, conjugated olefins	9.0–6.0	13.00	15.58	27.49

Elemental compositions of column chromatographic subfractions of bio-oil are shown in Table 4. H/C ratio of the n-pentane subfraction of oil was 1.65 and this number is close to the values of standard diesel. Calorific values of aliphatic subfractions are significantly higher than that of aromatic and polar subfractions, and aliphatic subfraction from steam pyrolysis has the highest calorific value as expected. All subfractions have low oxygen content and high H/C ratios than the both original feedstock and bio-oils.

Bio-oils obtained under optimum conditions were separated into n-pentane soluble and asphaltenes. The n-pentane soluble parts were further fractionated by adsorption chromatography. The results of adsorption chromatography of the oils show that the pyrolyzed oil under static, nitrogen, and steam atmospheres consists of 48%, 50%, and 65% of n-pentane solubles, respectively. Maltenes (n-pentane soluble part of oils) increases whereas asphaltenes decreases after steam pyrolysis. The aliphatic, aromatic, and polar fractions of the oil under static atmosphere are 17%, 35%, and 48%, under steam atmosphere these fractions are found as 30%, 45%, and 25%, respectively. There is an increment in the aliphatic and aromatic fractions of the oil obtained under steam atmosphere, which is favorable for the production of fuels and chemicals.

Table 4. Elemental compositions and calorific values of subfractions from column chromatography for the bio-oils obtained at 600°C.

	Static (%)			Nitrogen (%)			Steam (%)		
Component	Aliphatic	Aromatic	Polar	Aliphatic	Aromatic	Polar	Aliphatic	Aromatic	Polar
C	82.53	71.39	66.79	85.30	77.29	63.85	86.10	69.04	64.23
H	13.68	9.72	8.75	13.67	9.47	8.60	13.56	8.03	8.86
N	0.60	0.55	–	1.14	–	0.17	0.34	–	0.18
O[a]	3.19	18.54	24.46	–	13.24	27.75	–	22.94	26.65
H/C	1.99	1.63	1.57	1.92	1.47	1.62	1.89	1.45	1.62
Calorific value (MJ kg^{-1})	47.08	34.87	30.81	48.58	35.67	29.00	48.63	30.81	29.70

[a]By difference.

Table 5. Results of FTIR Spectra for Bio-Oils and Their Subfractions.

		Static				Nitrogen				Steam			
Band position (cm^{-1})	Assignment	Bio-oil	Aliphatics	Aromatics	Polars	Bio-oil	Aliphatics	Aromatics	Polars	Bio-oil	Aliphatics	Aromatics	Polars
3600–3400	ν (O-H)	+	–	+	+	+	–	–	+	+	–	+	+
3040–3000	ν(C-H)Aromatic ring	+	–	+	–	+	–	+	–	+	–	+	–
2980–2930	ν_{as}(C-H)	+	+	+	+	+	+	+	+	+	+	+	+
2870–2850	ν_{s}(C-H)	+	+	+	+	+	+	+	+	+	+	+	+
1720–1770	ν (C=O)	+	+	+	+	+	+	+	+	+	–	+	+
1625–1590	ν (C=C)	+	+	+	–	+	+	–	–	+	+	–	–
1600,1580,1450	Aromatic ring	+	+	+	–	+	+	+	+	+	–	+	+
1460	δ_{as} (CH_3, CH_2 scissor)	+	+	+	+	+	+	+	+	+	+	+	+
1375	δ_{s}(C-H)	+	+	+	+	+	+	+	+	+	+	+	+
1275–1200	ν_{as}(=C-O-C)	+	–	+	+	+	–	+	+	+	–	+	+
1150–1070	ν_{as}(C-O-C)/OHsecondary, OH primary	+	–	+	+	+	–	+	+	+	–	+	–
900–700	Substituents of aromatic ring	–	+	+	+	+	–	+	+	+	–	+	+
740–720	γ(C-H)	+	+	+	+	+	+	+	+	+	+	+	+
730–675	γ(=CH)	+	+	+	+	+	+	–	+	–	+	+	+
720–725	Rocking band	+	–	+	+	+	+	–	–	–	+	–	–

Table 5 shows the results of FTIR spectra of the bio-oils and its subfractions. Biomass pyrolysis oils contain a very wide range of complex organic chemicals (Savova et al. 2001; Uzun et al. 2010). The O–H stretching vibrations between 3200 and 3400 cm^{-1} indicate the presence of water, carboxylic acids, phenols, and alcohols. Table 5 shows that no peak exists between these wave numbers for the aliphatic subfraction of bio-oil, and this indicates that aliphatic subfraction does not contain oxygenated compounds like bio-oil, and this result obtained in the present study was also in consistent with elemental and GC/MS analysis. The C–H stretching vibrations between 2850 and 2925 cm^{-1} and C–H deformation vibrations between 1350 and 1475 cm^{-1} indicate the presence of alkanes. Moreover, the location of bending vibration of C–H groups at 1378 cm^{-1} provides another evidence of the fact that this band is very important for the detection of methyl groups in a given compound. Carbonyl stretching absorptions cause the band at about 1745 cm^{-1} in the spectrum. In addition, the presence of these peaks together with the presence of C=C stretching vibrations between 1680 cm^{-1} and 1700 cm^{-1} is compatible with the presence of ketone, quinone, aldehyde groups, etc. Aromatic ring C–H stretching vibration 3000 cm^{-1} and stretching vibration of aliphatic bonding to the aromatic ring at 2923 cm^{-1} are an important evidence of the aromaticity of toluene subfraction.

The aliphatic subfractions of pentane subfractions are obtained under static, nitrogen, and steam atmospheres. Aliphatic subfractions consist of n-alkanes, alkenes, and branched hydrocarbons. The abundances of the products are listed and compared in Table 6 by a semi-quantitative study made by means of the percentage of area of the chromatographic peaks. The majority of the linear chain hydrocarbons were distributed in the range of C_{12}–C_{31} but the intensive peak can be considered as C_{12}–C_{18}. When compared with standard diesel, it is obviously seen that the distribution of

Table 6. Relative Proportions (Area%) of Main Pyrolysis Compounds in the Aliphatic Subfraction of Bio-Oils.

		%Area		
Compound	Retention time	Static	Nitrogen	Steam
1-Dodecene	7.47	2.10	–	–
Tridecane	14.38	–	0.97	–
1-Tetradecene	15.64	13.68	1.94	–
Tetradecane	15.78	–	2.91	
1-Pentadecene	17.10	–	1.46	–
Pentadecane	17.27	2.10	4.37	–
1-Tridecene	18.74	–	0.97	–
1-Hexadecene	18.76	17.89	–	–
Hexadecane	18.92	–	2.91	–
7-Hexadecene	18.93	1.58	–	–
Heptadecane	20.83	–	2.43	–
1-Octadecene	22.83	22.11	–	–
Octadecane	23.04	–	1.94	–
N-Nonadecane	25.57	–	13.11	–
Eicosane	28.40	35.79	10.19	11.83
Heneicosane	31.50	–	19.42	16.03
1-Docosene	34.49	4.74	–	–
Docosane	34.79	–	4.85	–
Tricosane	38.20	–	5.34	–
Tetratriacontane	39.83	–	–	19.46
Tetracosane	41.69	–	7.28	–
Hexacosane	48.67	–	10.67	23.28
Eicosane, 9-octyl-	44.37	–	–	16.03
Pentacosane	45.19	–	9.22	–
Heptacosane	52.21	–	–	13.36

Table 7. Elemental Compositions and Calorific values of the Solid Products Obtained under Different Atmospheres at 600°C.

Component	Staticatmosphere (%)	Sweeping gasatmosphere (%)	Steamatmosphere (%)
C	71.94	80.57	86.87
H	1.76	1.38	0.73
N	0.97	0.79	0.62
O	25.33	17.25	11.78
H/C	0.29	0.21	0.10
Empirical formula	$CH_{0,29}N_{0,012}O_{0,01}$	$CH_{0,21}N_{0,008}O_{0,16}$	$CH_{0,10}N_{0,006}O_{0,1}$
Calorofic value (Mj kg^{-1})	22.31	26.141	28.31

hydrocarbons for n-pentane sub-fraction shows similarities with diesel. Considering the results of GC-MS detailed analysis, the percentage of alkanes is largest in oil obtained from steam pyrolysis due to the conversion of unsaturated hydrocarbons (alkenes) to saturated hydrocarbons (alkanes) while the desorption of low molecular products takes place during the process of steam pyrolysis.

Table 7 gives the results of elemental analyses of the solid products obtained under optimum conditions. Carbon content and calorific values are the important parameters for chars when they are used as either activated carbons or solid fuels. Indeed, slow pyrolysis seems to be a suitable way when high yields of the carbon-enriched solid product (char) are required. Char can be directly used as a fuel or submitted to further processing to produce more value-added chemicals, such as activated carbons. It can be seen from the table that char obtained under steam atmosphere is more useful for these purposes since its calorific value is higher than that of the two other chars. The char can also be used as a fuel when mixed with the liquid product (Bridgewater and Grassi 1991; Suarez-Garcia, Martinez-Alonso, and Tascon 2002; Uzun et al. 2010).

Table 8 shows the results of FTIR spectra of the bio-chars. The bands at about 3450–3350 cm^{-1} for all chars represent O–H vibrations in hydroxyl groups. Very weak bands at about 2850 cm^{-1} for 400°C and 450°C are assigned to C–H stretching vibrations in CH_2 groups. With increasing pyrolysis temperature, decreasing intensities of the bands between 2000 and 1500 cm^{-1} are ascribed to double bond vibrations for all types of aromatics. Chars obtained at higher temperatures contain little or no vibration bands at around 2900 cm^{-1} indicating that their aliphaticity is lower than the low temperature char. Previous studies for different biomass samples indicate that carbonization, especially at higher temperatures, increases the aromatic carbon content while decreasing aliphaticity (Bonelli et al. 2002; El-Hendawy 2006). Also, the presence of many weak bands in 400°C that are very similar to almond shell spectrum (Figure 1) is a good proof of uncompleted pyrolysis reactions at lower temperatures.

Conclusions

The experimental study showed that the pyrolysis atmosphere has important roles on the bio-oil yield and composition. Pyrolysis reactions are mainly affected by temperature. While the oil yield was 18.93% at a pyrolysis temperature of 400°C, it appeared to go through a maximum of 24.23% at the temperature of 600°C. It can be concluded that at higher temperatures above the optimum, the amount of bio-oil decreases due to gasification reactions, so higher temperatures are favored for obtaining gaseous products.

The presence of steam increases the oil and gas yields significantly, while solid yields decrease. This situation explained that the steam inhibits the secondary cracking reactions of the pyrolysis products. According to our results, the maximum bio-oil yield was achieved as 33.05%, under steam atmosphere as then steam velocity was 1.3 cm s^{-1}.

The spectroscopic results are consistent with the chromatographic data, confirming that the hydrocarbons of the n-pentane subfractions of all pyrolysis oils are the mixtures of alkanes and alkenes. The comparison of H/C ratios with conventional fuels has shown that the H/C ratios of the oils obtained in this work are between those of light and heavy petroleum products. Moreover, the FTIR analysis shows that the produced oil is a mixture of aliphatic, aromatic hydrocarbons and hydroxyl, carboxylic groups. According

Table 8. Result of FTIR Spectra for Bio-Chars.

Type of functional group	Wave number(cm^{-1})	400°C	450°C	500°C	550°C	600°C	700°C	N_2[a]	H_2O[b]
OH stretch	3600–3200	+	+	+	+	+	–	+	+
Aromatic ring stretching	3100–3000	+	+	+	+	+	–	+	+
ν_{as} (C-H)_ _	2960–2926	+	+	+	+	+	–	+	+
Aliphatics bonding with aromatic ring	2900–2900	+	+	+	+	+	–	+	+
ν_s(C-H)	2900–2870	+	+	+	+	+	+	+	+
Carbonyl	1718–1680	+	+	+	+	+	–	+	+
C=C stretch	1645	–	–	–	–	–	–	–	–
Aromatic C=C stretch	1610,1500,1420	+	+	+	+	+	+	+	+
δ_s	1465,1380	+	+	+	+	+	–	+	+
δ_{as}	1460–1450	+	+	+	+	+	–	+	+
C–O stretch	1270–1060	–	–	–	–	–	–	–	–
OH bending	1240	–	–	–	–	–	–	–	–
Ketone or ester bending	1120	–	–	–	–	–	–	–	–
Polycyclic heteroatoms	1100	–	–	–	–	–	–	–	–
In plane C–H bending	1080–1025	–	–	–	–	–	–	–	–
Substituents of aromatic ring	700–900	+	+	+	+	+	–	+	+
Out-of-plane CH bending	730	–	–	–	–	–	–	–	–
Rocking band	720–725	–	–	–	–	–	–	–	–
Out-of-plane =CH bending	698	–	–	–	–	–	–	–	–

[a]Obtained at 600°C, 5°C min^{-1}, sweeping gas flow rate of 100 cm^3 min^{-1}.
[b]Obtained at 600°C, 5°C min^{-1}, steam velocity of 1.3 cm s^{-1}.

to GC-MS and column chromatography results, steam pyrolysis can be used for indirect hydrogenation of evolved volatiles during the reaction.

The characterization depending on the structure analysis of the oil and fractions has shown that these fractions are quite similar to currently utilized transport fuels and can be utilized as transport fuels or chemical feed-stocks. Determination of suitable operating conditions such as pyrolysis temperature and atmosphere is very important to develop an adapted process for future demand.

References

Bellamy, L. J. 1975. *The infra-red spectra of complex molecules*. London: Chapman and Hall Ltd.

Bonelli, P. R., P. A. Della Rocca, E. G. Cerella, and A. L. Cukierman. 2002. Effect of pyrolysis temperature on composition, surface properties and thermal degradation rates of Brazil nut shells. *Bioresource Technology* 76:15–22.

Bridgewater, A. V. and G. Grassi. 1991. *Biomass pyrolysis liquids upgrading and utilisation*. England: Elsevier.

Bridgwater, A. V., D. Meier, and D. Radlein. 1999. An overview of fast pyrolysis of biomass. *Organic Geochemistry* 30:1479–93.

Caballero, J. A., R. Font, and A. Marcilla. 1996. Comparative study of the pyrolysis of almond shells and their fractions, holocellulose and lignin, product yields and kinetics. *Thermochimica Acta* 276:57–77.

Cornelissen, T., M. Jans, M. Stals, T. Kuppens, T. Thewys, and G. K. Janssens. 2009. Flash co-pyrolysis of biomass: the influence of biopolymers. *Journal of Analytical and Applied Pyrolysis* 85:87–97.

Demirbaş, A. 2006. Effect of temperature on pyrolysis products from four nut shells. *Journal of Analytical and Applied Pyrolysis* 76:285–9.

Duran-Valle, C. J., M. Gomez-Corzo, J. Pastor-Villegas, and V. Gomez-Serrano. 2005. Study of cherry stones as raw material in preparation of carbonaceous adsorbents. *Journal of Analytical and Applied Pyrolysis* 73:59–67.

Ekinci, E. and Y. Yurum. 1995. Steam and coprocessing of oil shales, In Composition, geochemistry and conversion of oil shales. NATO ASI Series, Vol. 455, C. Snape (ed.), Amstrdam: Springer. pp. 247–62.

El-Hendawy, A. A. 2006. Variation in the FT-IR spectra of a biomass under impregnation, carbonization and oxidation conditions. *Journal of Analytical and Applied Pyrolysis* 75:159–66.

Encinar, J. E., J. F. Gonzales, and J. Gonzales. 2000. Fixed-bed pyrolysis of Cynara Cardunculus L. Product yields and compositions. *Fuel Processing Technology* 68:209–22.

Font, R., A. Marcilla, A. N. Garcia, J. A. Caballero, and J. A. Conesa. 1995. Comparison between the pyrolysis products obtained from different organic wastes at high temperatures. *Journal of Analytical and Applied Pyrolysis* 32:41–9.

Font, R., A. Marcilla, E. Verdu, and J. Devesa. 1986. Fluidized-bed flash pyrolysis of almond shells. Temperature influence and catalysts screening. *Industrial and Engineering Chemistry Product Research and Development* 25:496–9.

Fukuda, S. 2015. Pyrolysis investigation for bio-oil production from various biomass feedstocks in Thailand. *International Journal of Green Energy* 12:215–24.

Gokcol, C. B., B. Dursun, E. Alboyaci, and E. Sunan. 2009. Importance of biomass energy as alternative to other sources in Turkey. *Energy Policy* 37:424–31.

Gonzalez, J. F., Ramiro, A., Gonzalez-Garcia, C. M., Ganan, J. Encinar, J. M., and E. Sabio. 2005. Pyrolysis of almond shells. Energy applications of fractions. *Journal of Industrial and Engineering Chemistry* 44:3003–12.

Harker, J. H. and J. R. Backhurst. 1981. *Fuel and energy*. London: Academic Press Limited.

Jenkins, B. M., A. D. Jones, S. Q. Turn, and R. B. Williams. 1996. Emission factors for polycyclic aromatic hydrocarbons from biomass burning. *Environmental Science and Technology* 30:2462–69.

Jin, L., L. Wang, L. Su, and Q. Cao. 2012. Characteristics of gases from co-pyrolysis of sawdust and tires. *International Journal of Green Energy* 9:719–30.

Minkova, V., M. Razvigorava, E. Bjornbom, R. Zanzi, T. Budinova, and N. Petrov. 2001. Effect of water vapour and biomass nature on the yield and quality of the pyrolysis products from biomass. *Fuel Processing Technology* 70:53–61.

Minkova, V., M. Razvigorava, M. Goronova, L. Ljutzkanov, and G. Angelova. 1991. Effect of water vapour on pyrolysis of solid fuels. *Fuel* 70:713–9.

Mohan, D., C. U. Pittman,and P.H. Steele. 2006. Pyrolysis of wood/biomass for bio-oil: A critical review. *Energ. Fuels* 20:848–89.

Mohan, D., A. Sarswat, V. K. Singh, M. A. Franco, and C. U. Pittman Jr. 2011. Development of magnetic activated carbon from almond shells for trinitrophenol removal from water. *Chemical Engineering Journal* 172:1111–25.

Nabais, J. M. V., C. E. C. Laginhas, P. J. M. Carrott, and M. M. L. Ribeiro. 2011. Production of activated carbons from almond shell. *Fuel Processing Technology* 92:234–40.

Önal, E. P., B. B. Uzun, and A. E. Pütün. 2011. Steam pyrolysis of an industrial waste for bio-oil production. *Fuel Processing Technology* 92:879–85.

Pindoria, R. V., J. Y. Lim, J. E. Hawkes, M. J. Lazaro, A. A. Herod, and R. Kandioti. 1997. Structural characterization of biomass pyrolysis tars/oils from eucalyptus wood waste: Effect of H_2 pressure and sample configuration. *Fuel* 76:1013–23.

Pütün, A. E., A. Ozcan, and E. Pütün. 1999. Pyrolysis of hazelnut shells in a fixed-bed tubular reactor: Yields and structural analysis of bio-oil. *Journal of Analytical and Applied Pyrolysis* 52:33–49.

Pütün, E., B. B. Uzun, and A. E. Pütün. 2006. Fixed-bed catalytic pyrolysis of cotton-seed cake: Effects of pyrolysis temperature, natural zeolite content and sweeping gas flow rate. *Bioresource Technology* 97:701–10.

Savova, D., E. Apak, E. Ekinci, F. Yardım, N. Petrov, and T. Budinova. 2001. Biomass conversion to carbon adsorbent and gas. *Biomass and Bioenergy* 21:133–42.

Suarez-Garcia, F., A. Martinez-Alonso, and J. M. D. Tascon. 2002. Pyrolysis of apple pulp: Effect of operation conditions and chemical additives. *Journal of Analytical and Applied Pyrolysis* 62:93–109.

Uzun, B. B., E. Apaydin-Varol, F. Ates, N. Ozbay, and A. E. Pütün. 2010. Synthetic fuel production from tea waste: Characterization of bio-oil and bio-char. *Fuel* 89:176–84.

Uzun, B. B., A. E. Pütün, and E. Pütün. 2007. Rapid pyrolysis of olive residue. 1. Effect of heat and mass transfer limitations on product yields and bio-oil compositions. *Energy and Fuels* 21:1768–76.

Uzun, B. B., A. E. Pütün, and E. Pütün. 2007. Composition of products obtained via fast pyrolysis of olive-oil residue: Effect of pyrolysis temperature. *Journal of Analytical and Applied Pyrolysis* 79:147–53.

Vitolo, S., M. Seggiani, P. Frediani, G. Ambrosini, and L. Politi. 1999. Catalytic upgrading of pyrolytic oils to fuel over different zeolites. *Fuel* 78:1147–59.

Wang, S., Q. Liu, K. Wang, X. Guo, Z. Luo, K. Cen, and T. Fransson. 2010. Study on catalytic pyrolysis of manchurian ash for production of bio-oil. *International Journal of Green Energy* 7:300–9.

Williams, P. T. and S. Beşler. 1992. The pyrolysis of rice husks in a thermogravimetric analyzer and static batch reactor. *Fuel* 73:151–9.

Zhang, Q., T. Wang, C. Wu, L. Ma, and Y. Xu. 2010. *Fractioned preparation of bio-oil by biomass vacuum pyrolysis*. *International Journal of Green Energy* 7:263–72.